Proceedings of the ASME 2015 Dynamic Systems and Control Conference
DSCC2015
October 28-30, 2015, Columbus, Ohio, USA

DSCC2015-9660

MOTION PLANNING AND DIFFERENTIAL FLATNESS OF MECHANICAL SYSTEMS ON PRINCIPAL BUNDLES

Tony Dear*
Robotics Institute
Carnegie Mellon University
Pittsburgh, Pennsylvania 15213
tonydear@cmu.edu

Scott David Kelly
Department of Mechanical Engineering
and Engineering Science
University of North Carolina at Charlotte
Charlotte, North Carolina 28223
scott@kellyfish.net

Matthew Travers **Howie Choset**
Robotics Institute
Carnegie Mellon University
Pittsburgh, Pennsylvania 15213
mtravers@andrew.cmu.edu,
choset@cs.cmu.edu

ABSTRACT

Mechanical systems often exhibit physical symmetries in their configuration variables, allowing for significant reduction of their mathematical complexity arising from characteristics such as underactuation and nonlinearity. In this paper, we exploit the geometric structure of such systems to explore the following motion planning problem: given a desired trajectory in the workspace, can we explicitly solve for the appropriate inputs to follow it? We appeal to results on differential flatness from the nonlinear control literature to develop a general motion planning formulation for systems with symmetries and constraints, which also applies to both fully constrained and unconstrained kinematic systems. We conclude by demonstrating the utility of our results on several canonical mechanical systems found in the locomotion literature.

INTRODUCTION

In the analysis of mechanical systems, one often desires to express the equations of motion in a manner conducive to analysis and control. For a certain class of systems, this motivation often amounts to *reducing* the equations by exploiting a system's natural symmetries and the corresponding invariants due to Noether's theorem. The configuration variables of such systems often constitute a principal fiber bundle structure defined by a Lie group (the non-actuated symmetry directions) and a shape manifold (the system's actuated internal configuration). For example, the two-wheeled mobile robot shown in Fig. 1 locomotes on the plane, parameterized by the Lie group $SE(2)$ (position and orientation of the robot), and has a shape manifold parameterized by its two wheel angles ψ_1 and ψ_2.

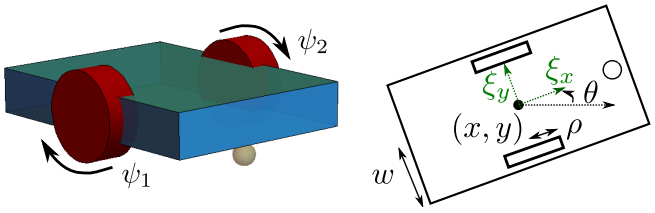

FIGURE 1: TWO-WHEEL DIFFERENTIAL-DRIVE CAR.

In recent years, many results have analyzed the properties and structure of the reduced equations that emerge from such a splitting. These formulations have been shown to accommodate nonholonomic constraints as well as locomotion in high and low Reynolds number fluids. The equations' structure, and in particular the kinematic form, has been shown to be conducive to the analysis of forward motion planning, which has found much success in periodic inputs known as gaits.

In this paper, we attack the motion planning problem head-on; instead of deriving gaits to achieve a desired motion, we are interested in situations for which the inputs can be directly solved to follow a complete trajectory in the position variables. This problem bears similar overtones to that of exploiting differential flatness in systems theory, a property useful for trajec-

*Address all correspondence to this author.

tory planning for nonlinear dynamical systems. To the authors' knowledge, commonalities between these systems and those with reducible geometric structure have been little explored in the locomotion literature, and here we try to clarify some of these links in the motion planning context.

We structure our paper as follows. We first present an overview of relevant work in the geometric mechanics and differential flatness communities. Following this, we present the necessary mathematical tools and summarize relevant results from prior work. In the next section, we explicitly state the motion planning problem and present the general solution for mixed nonholonomic systems followed by the special cases of principally kinematic and purely mechanical systems. We finish by considering the specific case of systems on $SE(2)$ and applying our technique to several examples from the literature.

PRIOR WORK

Much of the early work in the geometric mechanics of locomotion characterized systems with bundle structures, and in particular those with symmetries and constraints. Kelly and Murray [1] approached locomotion as a consequence of geometric phase due to gaits on a manifold and also discussed the issue of controllability. Bloch et al. [2] considered systems subject to both symmetries and nonholonomic constraints, detailing their effects on the corresponding momentum laws. Ostrowski [3] explicitly presented the derivations of the reduced equations and categorized systems as either kinematic or mixed (dynamic).

The notion of a connection that determines the position outputs of a system in response to shape inputs lends itself to gait analysis for motion planning, as shown in earlier work by Ostrowski et al. for the snakeboard [4] and later extended to optimal gait search [5]. Mukherjee and Anderson [6, 7] were able to perform integration of the connection using Stokes' theorem to develop gaits for the rolling disk, and Melli et al. [8] did so for a three-link swimmer. Shammas et al. [9, 10] exploited the structure of the connection and developed the use of height functions to systematically evaluate the efficacy of gaits in the shape space. This work was extended by Hatton and Choset [11] to extract more accurate evaluations via coordinate optimization.

Given an input trajectory, the analysis of gaits can yield information on a system's possible output motions and trajectories. But it may be difficult to solve the reverse problem of deriving an input from an arbitrary output, addressed as a result of the differential flatness property of control systems. The theory of differential flatness was introduced by Fliess et al. [12] and Martin et al. [13]; Murray et al. [14] enumerated a canonical catalog of differentially flat systems. Examples of analytical trajectory generation were shown for trailer systems [15] and towed cables [16], among others. Finally, application of nonlinear control to mechanical systems was explored by Murray [17] and Bloch [18], including some discussion on trajectory generation.

MATHEMATICAL BACKGROUND

In this section we provide a brief summary of relevant developments from Lagrangian mechanics and geometric reduction. Once we have established the scope of the systems analyzed in this paper, we bring in the necessary concepts from dynamical systems and differential flatness, allowing us to explicitly detail the link between the two perspectives. More complete references for the first subject can be found in [1–4, 9, 10]; the second is discussed more extensively in [12–14, 19].

Lagrangian Mechanics

A mechanical system can be described by n configuration coordinates $q \in Q$. We can also associate with any system a Lagrangian $L : TQ \to \mathbb{R}$, defined as the difference between the system's kinetic and potential energy. It can be written as

$$L(q,\dot{q}) = \frac{1}{2}\dot{q}^T M(q)\dot{q} - V(q), \tag{1}$$

where $M(q)$ is the mass matrix and $V(q)$ is the potential energy.

A system can also be subject to a set of k linearly independent nonholonomic constraints. As in previous literature, we assume that such constraints can be written in *Pfaffian form* as

$$\omega(q)\dot{q} = 0. \tag{2}$$

Here $\omega(q)$ is a full row rank k by n matrix function of q; the constraint equations are linear in the velocities $\dot{q}$.

From this information, one can then generate the Euler-Lagrange equations of motion:

$$\frac{d}{dt}\left(\frac{\partial L(q,\dot{q})}{\partial \dot{q}_i}\right) - \frac{\partial L(q,\dot{q})}{\partial q_i} + \sum_{j=1}^{k} \lambda_j \omega_{ji}(q) = \tau_i, \quad i = 1,\ldots,n. \tag{3}$$

Here we introduce k Lagrange multipliers λ to incorporate the constraint distribution. We assume second-order torque inputs to the system τ_i, but presently make no requirement that the system be fully actuated. These equations can then be rewritten explicitly as the Newton-Euler equations as

$$M(q)\ddot{q} + C(q,\dot{q})\dot{q} + N(q,\dot{q}) = \tau. \tag{4}$$

The Coriolis matrix $C(q,\dot{q})$ contains the Coriolis and centrifugal contributions, while $N(q,\dot{q})$ includes all external forces, conservative and non-conservative.

Geometric Reduction

The configuration manifold Q of many mechanical systems can be expressed in a principal fiber bundle structure whereby a

certain subset of the variables collectively represents an element of a Lie group G. For a physical system, these *fiber variables* often specify an element of $SE(3)$—or some subgroup thereof—that encodes the system's position and orientation relative to a laboratory frame of reference. The system's internal configuration is described by the remaining coordinates that specify a point on a *shape* or *base manifold* M, allowing for a decomposition of the form $Q = G \times M$. Recall that Q has dimension n, and we now assume we have m actuated shape variables and l unactuated fiber variables, so that $n = l + m$.

We are now in a position to exploit the natural symmetries of the system to reduce the equations of motion to a more manageable form. We assume that the systems of interest have Lagrangians and constraints that are invariant under translation in the group variables $g \in G$; in other words, neither $L(q,\dot{q})$ nor $\omega(q)$ has explicit dependences on inertial position and orientation. Hence we can equivalently specify these functions at $g = e$, the identity element of the group, by defining

$$\xi = (T_e L_g)^{-1} \dot{g}, \tag{5}$$

where $T_e L_g : T_e G \to T_g G$ and $\xi \in T_e G$ is an element of the tangent space of e. More specifically, the elements ξ form the Lie algebra $\mathfrak{g}$ associated with G, and they correspond to velocities written in a body-fixed frame.

We can define the *reduced Lagrangian* in terms of the shape variables $r \in M$ and the configuration velocities $\dot{q} = (\xi, \dot{r})$ as

$$l(r,\xi,\dot{r}) = \frac{1}{2} \begin{pmatrix} \xi^T & \dot{r}^T \end{pmatrix}^T \hat{M}(r) \begin{pmatrix} \xi \\ \dot{r} \end{pmatrix} - V(r), \tag{6}$$

where the *reduced mass matrix* $\hat{M}(r)$ can be subdivided into the following components as follows:

$$\hat{M}(r) = \begin{pmatrix} I(r) & I(r)A(r) \\ A^T(r)I^T(r) & m(r) \end{pmatrix}. \tag{7}$$

$I(r)$ and $A(r)$ are the local forms of the locked inertia tensor and mechanical connection, respectively. Note that all components are functions of the shape variables only. We can perform a similar reduction and decomposition of the constraints (2), which become

$$\tilde{\omega}_\xi(r)\xi + \tilde{\omega}_r(r)\dot{r} = 0. \tag{8}$$

Reduced Equations of Motion

To proceed in deriving the reduced equations of motion, we introduce the *generalized nonholonomic momentum* as the projection of $\frac{\partial l}{\partial \xi}$ onto the null space of $\tilde{\omega}_\xi$, which encompasses the allowable directions of motion. Denoting this by $\Omega(r)$, we have

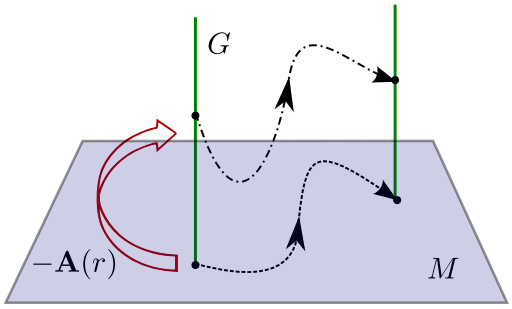

FIGURE 2: MAPPING BETWEEN BASE VELOCITIES AND FIBER VELOCITIES VIA THE CONNECTION FORM.

$$p = \left\langle \frac{\partial l}{\partial \xi}; \Omega \right\rangle = \Omega^T (I\xi + IA\dot{r}) := \eta_\xi(r)\xi + \eta_r(r)\dot{r}. \tag{9}$$

Hence p is a linear function in the configuration velocities, with coefficient matrices $\eta_\xi(r)$ and $\eta_r(r)$. For a system with k linearly independent constraints, p has dimension $l - k$.

Rewriting Eqn. (9) along with the reduced constraint equations (8), we can stack them together to find the following *reconstruction equation* for ξ:

$$\xi = -\begin{pmatrix} \tilde{\omega}_\xi \\ \eta_\xi \end{pmatrix}^{-1} \begin{pmatrix} \tilde{\omega}_r \\ \eta_r \end{pmatrix} \dot{r} + \begin{pmatrix} \tilde{\omega}_\xi \\ \eta_\xi \end{pmatrix}^{-1} \begin{pmatrix} \mathbf{0} \\ p \end{pmatrix} := -\mathbf{A}(r)\dot{r} + \Gamma(r)p. \tag{10}$$

Here $\mathbf{A} : T_r M \to \mathfrak{g}$ is the local form of the mixed nonholonomic connection, which relates changes in shape to changes in position. This relationship is shown graphically in Fig. 2, where a trajectory in M is mapped into a trajectory through the fibers corresponding to each traversed base configuration. The $l \times (l-k)$ matrix $\Gamma(r)$ is defined to be the rightmost $l-k$ columns of the matrix inverse on the left side. It is shown in [10] that this inverse indeed always exists.

The equation governing the evolution of p can be derived by differentiating the leftmost side of (9) and substituting into the Euler-Lagrange equations (3). The derivation is somewhat lengthy and is done in detail in [4, 10]. We state the result here, noting that it is quadratic in $\dot{r}$ and p:

$$\dot{p}_c = \dot{r}^T \sigma_{rr,c}(r)\dot{r} + \dot{r}^T \sigma_{rp,c}(r)p + p^T \sigma_{pp,c}(r)p. \tag{11}$$

Each of the σ matrices above is a matrix-valued function of r, derived from components of the reduced mass matrix, constraints, and reconstruction equation. We index Eqn. (11) above with c to indicate that there are $l-k$ evolution equations, one for each

component of p. These equations can also be stacked together to form one system of differential equations, with the σ matrices becoming third-order tensors.

Finally, the dynamics of the shape variables can be written in the second-order Newton-Euler form as in Eqn. (4). It can be shown that they constitute m equations of the form

$$\tilde{M}(r)\ddot{r}+\tilde{C}(r,\dot{r})\dot{r}+\tilde{N}(r,\dot{r},p)=\tau_r, \tag{12}$$

such that neither the mass matrix nor the Coriolis matrix depends on p. Taken together, Eqns. (10), (11), and (12) constitute the reduced dynamic equations of motion.

Note that if $k=m$, the constraints fully span the fiber space and Ω becomes trivial. Then the momentum p vanishes and we have a principal kinematic connection derived solely from constraints:

$$\xi=-\tilde{\omega}_\xi^{-1}(r)\tilde{\omega}_r(r)\dot{r}:=-\mathbf{A}_{\text{kin}}(r)\dot{r}. \tag{13}$$

A similar derivation occurs if there are no constraints and the initial momentum of the system is 0. In that case the reconstruction equation becomes purely mechanical:

$$\xi=-\eta_\xi^{-1}(r)\eta_r(r)\dot{r}:=-\mathbf{A}_{\text{mech}}(r)\dot{r}, \tag{14}$$

where we term $\mathbf{A}_{\text{mech}}(r)$ the mechanical connection. In both cases we no longer need the momentum evolution equation, leaving us with l first-order equations for the fiber variables and m second-order equations for the shapes.

Dynamical Systems and Differential Flatness

In the controls literature, one is often concerned with dynamical systems of the form

$$\dot{x}=f(x,u), \tag{15}$$

where x makes up the states of the system and u makes up the control inputs. Such a system is said to be *differentially flat* if there exist outputs y, with the same dimension as u, of the form $y=y(x,u,\dot{u},\ddot{u},\cdots,u^{(R)})$ such that the states and inputs can be expressed as functions of finite derivatives of the outputs, i.e.,

$$x=x(y,\dot{y},\ddot{y},\cdots,y^{(S)}), \tag{16}$$

$$u=u(y,\dot{y},\ddot{y},\cdots,y^{(S)}). \tag{17}$$

Here R and S must be finite integers. If such flat outputs exist for a system, then desired trajectories in the output space can be mapped directly to the inputs that produce them.

A more general concept, known as *partial differential flatness*, was introduced in [19]. For a system to possess this property, it is sufficient for a subset of the states and all the inputs to satisfy Eqns. (16) and (17). The dynamics of the non-flat states x_{nf} must be expressible as chains of integrators such that their trajectories can be found by integrating through functions of the flat outputs and their derivatives, i.e.,

$$x_{\text{nf},i}^{(M)}=h_i(y,\dot{y},\cdots,y^{(N)}). \tag{18}$$

As before, M and N must be finite integers. Thus, even though it may not be possible to analytically find all the states of partially flat systems, one can still do so numerically by integration.

For the purposes of defining a similar concept for systems on principal bundles, we note that the reduced equations can also be written in state space form. If we define our states as the $2n-k$ variables $x=(g,p,r,\dot{r})^T$ and the inputs as $u=\tau_r$, then

$$\dot{x}=\begin{pmatrix} T_eL_g(-\mathbf{A}(r)\dot{r}+\Gamma(r)p) \\ \dot{r}^T\sigma_{rr}(r)\dot{r}+\dot{r}^T\sigma_{rp}(r)p+p^T\sigma_{pp}(r)p \\ \dot{r} \\ -\tilde{M}^{-1}(r)(\tilde{C}(r,\dot{r})\dot{r}+\tilde{N}(r,\dot{r},p)) \end{pmatrix}+\begin{pmatrix} 0 \\ 0 \\ 0 \\ \tilde{M}^{-1}(r) \end{pmatrix}\tau_r. \tag{19}$$

Again, for kinematic systems we can eliminate p from the state, leaving $l+2m$ equations.

MOTION PLANNING: THE GENERAL CASE

For the general motion planning solution to the system (19), we would like to solve for the inputs τ_r given a desired trajectory in the workspace. While we cannot establish any differential flatness properties without looking at special cases, such as one described in the next section, we can still use similar ideas to guide the general solution. We will restrict ourselves to systems with an equal number of shape and fiber variables, i.e. $m=l$. The "outputs" that we would like to be able to command are the fiber variables g. If we are given g, then we can obtain $\dot{g}$ by differentiation, and we can freely transform into ξ and back using Eqn. (5). Hence we would like to show that there is a way to solve for τ_r using this information only.

Lemma 1. *Suppose that $\xi(t)$, differentiable, is given and that both $\xi(t)$ and $r(t)$ have dimension l. If the system is subject to k nonholonomic constraints, then $r(t)$ must satisfy $l-k$ second-order differential equations of the form*

$$\rho_1(r)\ddot{r}+\dot{r}^T\rho_2(r)\dot{r}+\dot{r}^T\rho_3(r)\xi+\rho_4(r,\xi,\dot{\xi})=0. \tag{20}$$

Proof. We first differentiate the RHS of Eqn. (9) to obtain a sys-

tem of $l-k$ differential equations. The cth equation is

$$\dot{p}_c = \eta_{r,c}(r)\ddot{r} + \dot{r}^T \frac{\partial \eta_{r,c}(r)}{\partial r}\dot{r} + \dot{r}^T \frac{\partial \eta_{\xi,c}(r)}{\partial r}\xi + \eta_{\xi,c}(r)\dot{\xi}, \quad (21)$$

where $\eta_{(\cdot),c}$ refers to the cth row of the respective matrix and $\partial \eta_{(\cdot),c}(r)/\partial r$ is the Jacobian matrix of the cth row of $\eta_{(\cdot)}$.

In addition, we can substitute Eqn. (9) into Eqn. (11) to obtain a first-order equation for $\dot{p}_c$ in terms of ξ, r and $\dot{r}$ only, shown below with the functional form (r) dropped for conciseness:

$$\begin{aligned}\dot{p}_c = \dot{r}^T(\sigma_{rr} + \sigma_{rp}\eta_r + \eta_r^T\sigma_{pp}\eta_r)\dot{r} + \xi^T\eta_\xi^T\sigma_{pp}\eta_\xi\xi \\ + \dot{r}^T(\sigma_{rp}\eta_\xi + \eta_r^T(\sigma_{pp}+\sigma_{pp}^T)\eta_\xi)\xi. \quad (22)\end{aligned}$$

Now equating the above two expressions for $\dot{p}_c$, we obtain Eqn. (20), where the cth row of each coefficient matrix is given by the following expressions, all functions of r.

$$\begin{aligned}\rho_1 &= \eta_{r,c}, \\ \rho_2 &= \frac{\partial \eta_{r,c}}{\partial r} - \sigma_{rr} - (\sigma_{rp} + \eta_r^T\sigma_{pp})\eta_r, \\ \rho_3 &= \frac{\partial \eta_{\xi,c}}{\partial r} - (\sigma_{rp} + \eta_r^T(\sigma_{pp}+\sigma_{pp}^T))\eta_\xi, \\ \rho_4 &= \eta_{\xi,c}\dot{\xi} - \xi^T\eta_\xi^T\sigma_{pp}\eta_\xi\xi. \end{aligned} \quad (23)$$

Note that while the expressions in (23) are matrices of varying sizes, Eqn. (20) is a scalar equation when everything is multiplied out. Hence each of the $l-k$ equations can be stacked together to obtain one system of differential equations. □

Proposition 1. *Suppose that $\xi(t)$, differentiable, is given and that both $\xi(t)$ and $r(t)$ have the same dimesionality. Suppose also that zero- and first-order initial conditions for $r(t)$ are given. Then there exists a unique set of inputs $\tau_r(t)$ such that the system follows the trajectory $\xi(t)$.*

Proof. Starting with Lemma 1, we can obtain a set of $l-k$ equations in the form of (20). From the nonholonomic constraints (8), we have k further equations, linearly independent from those of (20). Hence we have a total of l differential equations in m unknowns. Since $m = l$ and we have the appropriate initial conditions for $r(t)$, we can numerically solve the equations for $r(t)$.

The shape dynamics are given in Eqn. (12), which gives τ_r as a function of r, $\dot{r}$ and p. Since we now know $r(t)$ and $\xi(t)$ as functions of time, we can find τ_r as follows:

$$\tau_r = \tilde{M}(r)\ddot{r} + \tilde{C}(r,\dot{r})\dot{r} + \tilde{N}(r,\dot{r},\eta_\xi(r)\xi + \eta_r(r)\dot{r}). \quad (24)$$

This illustrates our proposed method for motion planning. □

Discussion

The problem of solving for the input torques, given desired workspace trajectories, now comes down to solving for the shape variables, which can be done by solving the differential equations (8) and (20). In this method, we assumed that we have the same number of equations as unknowns, along with appropriate initial conditions for $r(t)$. We now briefly discuss some issues concerning the solutions for the shape variables, such as existence, uniqueness, and boundedness. We will also touch upon some possible simplifications to Eqn. (20), as well as the modifications necessary to accommodate non-fully actuated systems.

Characterization of Equations. Since the components of Eqs. (8) and (20) are derived from the system mass matrix and constraints, the nature of the solution of these equations depends on the system parameters. In particular, conditions like Lipschitz continuity [20], which is required of any general differential-algebraic system, carry over to Proposition 1 as well. As long as the provided $\xi(t)$ is also Lipschitz-continuous, a local unique solution can always be found numerically.

Unfortunately, there is currently no provision for the existence of a global solution to (8) and (20) in the general case. For example, it is shown in [21] that the required torque inputs to steer the snakeboard at a constant velocity grows without bound as the system approaches the singular configuration. While we cannot realistically use such solutions, we can still exploit the equations' structure to gain insight into the output limits of the system, as we will show in an example in the following section.

One advantage of working in this framework is that it is possible to establish conditions for when $r(t)$ can be solved explicitly without integration. Suppose that each of the equations turns out to be decoupled in the shape variables r. This may happen if the system states are physically decoupled from one another, if the system coordinates are defined such that each constraint is a function of one coordinate, or if the constraints pre-determine a subset of the solution independently of (20). If some of these conditions hold, the (partial) flatness of a system can be determined through the functional forms of these equations. Examples of special cases include ξ being constant (no dependence on t) or the symmetry directions being Abelian ($\sigma_{pp} = 0$) [4].

Another major simplification occurs when a system is kinematic, in which case the momentum p vanishes and the fibers of the system evolve according to either Eqn. (13) or (14). In this case, we only need to solve the first-order kinematic reconstruction equation for $r(t)$ given $\xi(t)$, and then propagate the shape dynamics through Eqn. (24). Assuming we have full actuation, the differential equation has the form

$$\dot{r}(t) = -\mathbf{A}(r(t))^{-1}\xi(t), \quad (25)$$

which can be solved by either quadrature or numerical integra-

tion. The usage of connection vector fields in conjunction with Stokes' theorem by Hatton and Choset [11] was applied to the goal of maximizing displacement in specific fiber directions.

Overactuated and Underactuated Systems. The technique described here cannot be directly applied to systems that are either over- or underactuated, relative to the number of fiber variables. In the former case we do not have enough equations and $l < m$; in the latter case we have too many equations and $l > m$. Both cases have been studied extensively for different motion planning techniques in the literature; here, we will simply look at kinematic systems.

For non-fully actuated kinematic systems, the local connection form is not bijective and the inverse does not exist. A simple solution is to use the left pseudoinverse, reminiscent of a similar technique for the Jacobians of redundant manipulators [22–24]:

$$\dot{r}(t) = -\mathbf{A}(r(t))^{+}\xi(t). \tag{26}$$

For overactuated systems, the solution will typically minimize the magnitudes of the shape variables. It is possible to optimize for more sophisticated criteria, for example by propagating the shape dynamics to find optimal torques; for general systems, this technique is addressed by control allocation [25, 26].

For underactuated systems, the solution will minimize the residual difference between the resultant fiber velocities $\hat{\xi}(t)$ and the desired $\xi(t)$; exact solutions are typically not possible, because the system's possible set of trajectories does not span the entire fiber space. Alternatively, one can specify a subset of desired fiber velocities; Eqs. (8) and (20) will then give the restrictions on the remaining ones. We will show an example of this in the next section.

MOTION PLANNING ON $SE(2)$

In this section we focus exclusively on systems on $SE(2)$, the group of planar rigid motions. The motivation for this particular class of systems is twofold: first, $SE(2)$ covers a large range of mechanical systems, many of which are wheeled mobile robots (WMRs); second, trajectories in $SE(2)$ have an intuitive correspondence to the system body velocities ξ, allowing us to show explicit examples of our motion planning techniques.

$SE(2)$ can be parameterized by the three coordinates $g = (x, y, \theta)$, where x and y denote the global position of the system and θ denotes its orientation. The transformation between body velocities ξ and world velocities $\dot{g}$ is given by

$$\xi = \begin{pmatrix} \xi_x \\ \xi_y \\ \xi_\theta \end{pmatrix} = \begin{pmatrix} \cos\theta & \sin\theta & 0 \\ -\sin\theta & \cos\theta & 0 \\ 0 & 0 & 1 \end{pmatrix} \begin{pmatrix} \dot{x} \\ \dot{y} \\ \dot{\theta} \end{pmatrix}. \tag{27}$$

Trajectories and Body Velocities

Given a desired trajectory $c(t) = (x(t), y(t), \theta(t))$, one can clearly find the equivalent body velocities by differentiation of $c(t)$ and substitution into (27). If we apply the restriction that $\tan\theta = \dot{y}/\dot{x}$, we show that ξ can be further written as explicit expressions of curvature and forward velocity. This requires that the robot is always oriented along its direction of motion, a reasonable assumption in many planning problems.

Given our constraint on θ, we can compute the following:

$$\cos\theta = \frac{\dot{x}}{v}, \quad \sin\theta = \frac{\dot{y}}{v}, \quad \dot{\theta} = \frac{\dot{x}\ddot{y} - \ddot{x}\dot{y}}{\dot{x}^2}\cos^2\theta = \kappa v, \tag{28}$$

where

$$v = \sqrt{\dot{x}^2 + \dot{y}^2}, \tag{29}$$

$$\kappa = \frac{\dot{x}\ddot{y} - \ddot{x}\dot{y}}{(\dot{x}^2 + \dot{y}^2)^{3/2}}. \tag{30}$$

Here v is the tangential velocity and κ is the curvature of the desired trajectory. Then it is straightforward to see that

$$\xi = \begin{pmatrix} \xi_x \\ \xi_y \\ \xi_\theta \end{pmatrix} = \begin{pmatrix} v(t) \\ 0 \\ \kappa(t)v(t) \end{pmatrix}, \tag{31}$$

where $c(t) = (\kappa(t), v(t))$ is an alternative parameterization of the desired trajectory to be tracked.

This form of trajectory representation affords us several advantages. It provides a simple relationship between the desired trajectory and corresponding body velocities, allowing one to easily find one side of (31) given the other. It reduces the number of relevant body velocity components to two, equal to the number of functions describing the trajectory. Finally, it allows us to characterize the types of trajectories that underactuated systems can follow, as there is an explicit relationship between the forward velocity ξ_x and turning rate ξ_θ.

Examples

Two-wheeled mobile robot. To illustrate the utility of working with the reduced equations of motion, we first look at the mobile robot in Fig. 1 detailed by Kelly and Murray [1]. It has two nonholonomically constrained wheels and a front caster for support, along with a wheel radius ρ and body half-width w. The system's shape manifold is parameterized by the two wheel angles $r = (\psi_1, \psi_2)^T$. We assume the wheel contacts on the ground to be governed by the pure rolling assumption and that a body frame is attached to a point equidistant from the wheels,

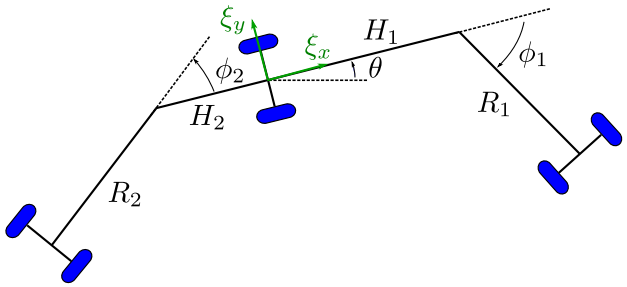

FIGURE 3: THREE-LINK KINEMATIC SNAKE ROBOT.

giving rise to three reduced constraints as follows:

$$\begin{pmatrix} 1 & 0 & 0 \\ 0 & 1 & 0 \\ 0 & 0 & 1 \end{pmatrix} \xi - \frac{\rho}{2} \begin{pmatrix} 1 & 1 \\ 0 & 0 \\ w^{-1} & -w^{-1} \end{pmatrix} \dot{r} = 0. \tag{32}$$

This system is principally kinematic, since the number of constraints is equal to the dimension of the group. The kinematic connection is trivially given as $\mathbf{A}_{\text{kin}} = \tilde{\omega}_r$, since $\tilde{\omega}_\xi$ is simply the identity mapping. From Eqn. (26), the shape variables can be solved according to the following differential equations:

$$\dot{r}(t) = \frac{1}{\rho} \begin{pmatrix} 1 & w \\ 1 & -w \end{pmatrix} \begin{pmatrix} v(t) \\ \kappa(t)v(t) \end{pmatrix}. \tag{33}$$

From this we can conclude that this system is partially differentially flat. Taking the flat outputs to be inertial coordinates x and y, we can find θ, κ, and v according to Eqns. (29) and (30), which then give us $\dot{r}$ according to the above equation. It is shown in [1] that the shape dynamics take the form $\tilde{M}\ddot{r} = \tau_r$, independent of r, allowing us to solve for the inputs τ_r without integration. The remaining, non-flat states are the shape variables r, which can be found by integrating Eqn. (33) above once.

Kinematic snake. The kinematic snake, detailed by Shammas et al. [9] and shown in Fig. 3, is a three-link robot with nonholonomically constrained wheels on each of its links; locomotion is achieved by actuating the two joints between the links. We assume that the links have lengths R_1, R_2, and $H_1 + H_2$ as shown, and that the shape manifold is parameterized by the two joint angles $r = (\phi_1, \phi_2)^T$. As with the two-wheeled car, there are exactly three constraints, making the system principally kinematic. Each of them is of the form

$$-\dot{x}_i \sin\theta_i + \dot{y}_i \cos\theta_i = 0, \tag{34}$$

where x_i, y_i, and θ_i are the global coordinates of the ith wheelset. x_2 and y_2 coincide with the body frame, so the constraints in

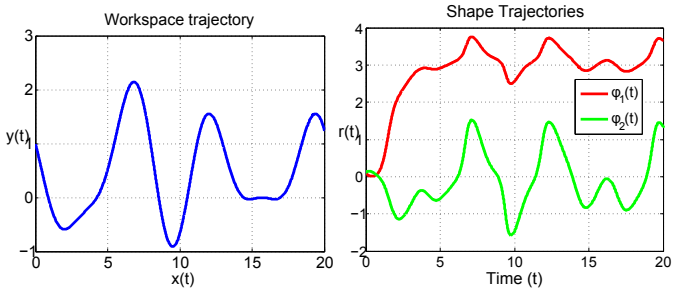

(a) (b)

FIGURE 4: (a) DESIRED WORKSPACE TRAJECTORY AND (b) CORRESPONDING JOINT INPUT ANGLES.

reduced form can be written as

$$\begin{pmatrix} \sin\phi_1 & \cos\phi_1 & H_1\cos\phi_1 + R_1 \\ 0 & 1 & 0 \\ -\sin\phi_2 & \cos\phi_2 & -H_2\cos\phi_2 - R_2 \end{pmatrix} \xi - \begin{pmatrix} R_1 & 0 \\ 0 & 0 \\ 0 & R_2 \end{pmatrix} \dot{r} = 0. \tag{35}$$

Unlike the previous example, the kinematic connection here $\mathbf{A}_{\text{kin}}$ depends on the shape variables r, as $\tilde{\omega}_\xi$ is not constant. Furthermore, it is not possible to solve the differential equations analytically for any arbitrary ξ. (We do note that if curvature is constant, we will have that $\xi_x = v(t) \propto \xi_\theta$, which may allow for an explicit solution by quadrature for ϕ_1 and ϕ_2 separately, since the equations are decoupled.) Instead, we rewrite the constraints into the form (26) as shown below to perform numerical integration, after which the shape trajectories can be pushed through the dynamics to obtain the input torques:

$$\dot{r}(t) = \begin{pmatrix} \frac{1}{R_1}\sin\phi_1 & \frac{H_1}{R_1}\cos\phi_1 + 1 \\ -\frac{1}{R_2}\sin\phi_2 & -\frac{H_2}{R_2}\cos\phi_2 - 1 \end{pmatrix} \begin{pmatrix} v(t) \\ \kappa(t)v(t) \end{pmatrix}. \tag{36}$$

For the following simulation, we assume link lengths with $R_1 = R_2 = 1$ and $H_1 = H_2 = 2$. We choose $H_i > R_i$ to allow the outer links to swing around toward the middle link if necessary—we do not assume any joint limits. Suppose we want to follow the relatively complex workspace trajectory shown in Fig. 4a. This may be provided by a high-level planner with the goal of avoiding obstacles or hitting checkpoints, for example. From this we can find the velocity and curvature parameterization according to Eqns. (29) and (30), and we can then solve Eqn. (36) to obtain the shape trajectories shown in Fig. 4b.

Note that the solution for $\phi_1(t)$, the joint at the front link, requires the joint to operate around π radians most of the time. This corresponds to swinging the front link around to coincide with the middle link (this can be physically accomplished if the links are at different heights off the ground) and oscillating around

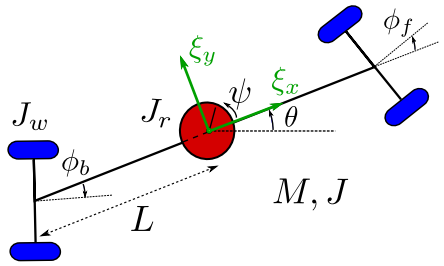

FIGURE 5: THE SNAKEBOARD.

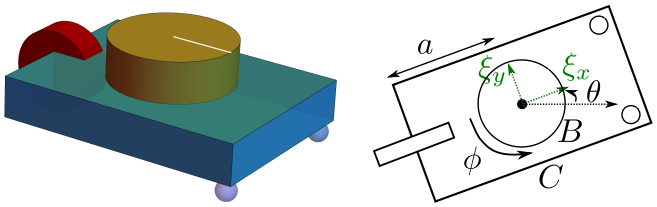

FIGURE 6: THE CHAPLYGIN BEANIE.

that configuration. In addition, neither of the joints is required to follow a periodic gait function. While we forego the geometric intuition afforded by height functions and connection vector fields, this direct method easily allows the robot to follow much more diverse trajectories than with previous techniques.

Snakeboard. Shown in Fig. 5, the snakeboard is an example of a mixed nonholonomic system that requires the use of Eqn. (23) to apply our motion planning formulation. This was the basis for the analysis done by Dear et al. [21]; here, we formulate it explicitly in terms of Proposition 1 and show that it is in fact a partially differentially flat system.

The snakeboard has mass M, length $2L$, and moment of inertia J; the rotor and wheelsets have inertias J_r and J_w, respectively, and we assume $ML^2 = J + J_r + 2J_w$. The system is actuated by two inputs, spinning the rotor at the center or rotating the wheelsets axles. These shape angles are denoted $r = (\psi, \phi)$; the wheel angles are locked to each other so that $\phi = \phi_f = -\phi_b$. The wheelsets give rise to two nonholonomic constraints, one fewer than the dimension of the fiber. With a body frame attached at the rotor, the reduced constraints take the form

$$\begin{pmatrix} -\sin\phi & \cos\phi & L\cos\phi \\ \sin\phi & \cos\phi & -L\cos\phi \end{pmatrix} \xi = 0. \tag{37}$$

Because these constraints can be subtracted to form a single algebraic equation in ϕ with no $\dot{\phi}$ or ψ terms, we can immediately solve them to obtain $\phi(t) = \tan^{-1}(L\xi_\theta/\xi_x)$. The fact that we are able to do this will be crucial in the next step.

As the number of constraints is fewer than the dimension of the fiber, we require the Lagrangian to account for the remaining symmetries not annihilated by the constraints.

$$l(\xi, \dot{r}) = \frac{1}{2}M(\xi_x^2 + \xi_y^2 + L^2\xi_\theta^2) + \frac{1}{2}J_r\dot{\psi}^2 + J_r\xi_\theta\dot{\psi} + J_w\dot{\phi}^2. \tag{38}$$

The derivation of the nonholonomic momentum and its evolution equation is detailed in [21]. We restate the results here and make explicit the components of Eqns. (9) and (11):

$$p = \begin{pmatrix} ML & 0 & ML^2\tan\phi \end{pmatrix}\xi + \begin{pmatrix} J_r\tan\phi & 0 \end{pmatrix}\dot{r}, \tag{39}$$

$$\dot{p} = \dot{r}^T \begin{pmatrix} 0 & J_r/2 \\ J_r/2 & 0 \end{pmatrix}\dot{r} + \dot{r}^T \begin{pmatrix} 0 \\ \tan\phi \end{pmatrix} p. \tag{40}$$

Now substituting each of these components into Eqn. (23), we obtain the differential equation

$$J_r\tan\phi\,\ddot{\psi} + \dot{r}^T \begin{pmatrix} 0 & -J_r/2 \\ J_r/2 & 0 \end{pmatrix}\dot{r} + \dot{r}^T \begin{pmatrix} 0 & 0 & 0 \\ -ML\tan\phi & 0 & ML^2 \end{pmatrix}\xi + \begin{pmatrix} ML & 0 & ML^2\tan\phi \end{pmatrix}\dot{\xi} = 0. \tag{41}$$

This is a second-order differential equation in ψ, which also contains terms in ϕ and $\dot{\phi}$. However, we already have an explicit solution for ϕ, and if we substitute this into Eqn. (41) along with the curvature parameterization of the fiber trajectory, we obtain

$$J_r\kappa(t)\ddot{\psi} + M\dot{v}(t) + ML^2\kappa(t)\frac{d}{dt}(\kappa(t)v(t)) = 0, \tag{42}$$

which is exactly the same equation used to solve for the rotor velocity $\dot{\psi}$ in [21].

Now taking this analysis one step further by finding the input torques, we can find the reduced shape dynamics by applying the Euler-Lagrange equations to Eqn. (38), with $\tau_r = (\tau_\psi, \tau_\phi)^T$.

$$\tau = \begin{pmatrix} J_r & 0 \\ 0 & 2J_w \end{pmatrix}\ddot{r} + J_r\ddot{\xi}_\theta. \tag{43}$$

Because the shape dynamics only require $\ddot{r}$, we can find the torque inputs without any integration—we get $\ddot{\psi}$ from Eqn. (42) and we can differentiate ϕ twice to obtain $\ddot{\phi}$. The snakeboard is therefore partially differentially flat. We are able to obtain ϕ and the input torques analytically provided the desired fiber outputs, while $\dot{\psi}$ and ψ can be found by simple integration of Eqn. (42), a known function of the desired outputs.

Chaplygin beanie. Our last example is the Chaplygin beanie, shown in Fig. 6 and introduced by Kelly et al. [27]. It is a mixed nonholonomic system with only one constraint on its back wheel; furthermore, it is severely underactuated with only one rotor input above its main platform. Despite these features, a simple method based on proportional control was presented in [27] to simultaneously propel and steer the system, though not independently. Due to underactuation, the beanie cannot follow any arbitrary fiber trajectory, but here we will be able to use our analysis to qualify feasible trajectories.

As done previously, we will derive the necessary equations using the reduced formulation. The one-dimensional shape manifold is parameterized by the rotor angle $r = \phi$, and the system has mass m and inertias B and C as shown; we will also denote the total inertia $J = ma^2 + B + C$. With the body frame attached to the center of the rotor, the constraint is simply

$$\begin{pmatrix} 0 & 1 & -a \end{pmatrix} \xi = 0. \tag{44}$$

Note that this gives us no information about ϕ, as the constraint acting on the system is completely decoupled from the rotor angle. We also require the Lagrangian to derive the momenta:

$$l(\xi, \dot{r}) = \frac{1}{2} m(\xi_x^2 + \xi_y^2) + \frac{1}{2} C \xi_\theta^2 + \frac{1}{2} B(\xi_\theta + \dot{\phi})^2. \tag{45}$$

The constraint is one-dimensional, which leaves us with a two-dimensional null space and hence two independent nonholonomic momenta. Their derivation can be found in [27]; here, we will rewrite the equations in reduced form, relabeling J_{LT} as p_1 and J_{RW} as p_2 and denoting $p = (p_1, p_2)^T$.

$$p = \begin{pmatrix} m & 0 & 0 \\ 0 & ma & B+C \end{pmatrix} \xi + \begin{pmatrix} 0 \\ B \end{pmatrix} \dot{r}, \tag{46}$$

$$\dot{p}_1 = \frac{maB^2}{J^2} \dot{r}^2 + \dot{r} \begin{pmatrix} 0 & \frac{-2maB}{J^2} \end{pmatrix} p + p^T \begin{pmatrix} 0 & 0 \\ 0 & \frac{ma}{J^2} \end{pmatrix} p, \tag{47}$$

$$\dot{p}_2 = \dot{r} \begin{pmatrix} \frac{ab}{J} & 0 \end{pmatrix} p + p^T \begin{pmatrix} 0 & -\frac{a}{2J} \\ -\frac{a}{2J} & 0 \end{pmatrix} p. \tag{48}$$

Now substituting the appropriate components from the above three equations into Eqn. (23), we obtain the following two differential-algebraic equations:

$$\dot{\xi}_x = a \xi_\theta^2, \tag{49}$$

$$B\ddot{\phi} = -(ma^2 + B + C)\dot{\xi}_\theta - ma\xi_x \xi_\theta. \tag{50}$$

Note that only the second of these two equations contains a term in the rotor acceleration. So given a feasible fiber trajectory, we can solve Eqn. (50) for $\ddot{\phi}$ and its integrals. The first equation gives an explicit condition on trajectory feasibility. In terms of velocity and curvature, this can be written as

$$\dot{v}(t) = a\kappa^2(t)v^2(t). \tag{51}$$

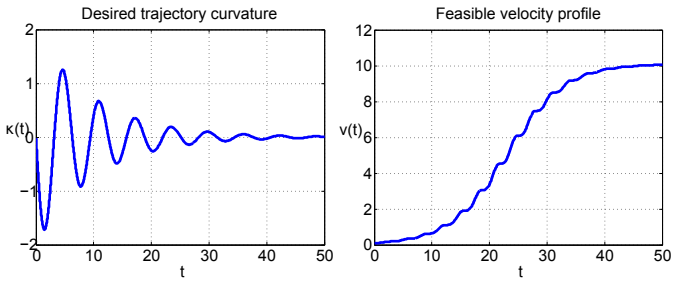

(a) (b)

FIGURE 7: (a) DESIRED TRAJECTORY CURVATURE AND (b) REQUIRED VELOCITY PROFILE.

In [27] it was shown that this system's trajectories evolve in a non-trivial manner. Eqn. (51) tells us precisely how steering and propulsion are coupled together. Given a particular path with a curvature parameterization $\kappa(t)$, the beanie's velocity must satisfy this equation, which can be solved as a nonlinear ordinary differential equation in $v(t)$.

Suppose that we wish to execute the fiber curvature function shown in Fig. 7a. Solving Eqn. (51) with all parameters set to 1, we find that the beanie must traverse such a path with a velocity profile shown in Fig. 7b; both functions agree roughly with the simulated trajectories in [27]. To derive the actual controller, we can then simply push the fiber velocities through Eqn. (50) to find $\ddot{\phi}$ and subsequently the corresponding input torque.

CONCLUSIONS AND FUTURE WORK

We have shown a novel approach to motion planning for a class of locomotion systems by exploiting their inherent fiber bundle structure and Lie group symmetries. Having provided desired fiber output trajectories, the required shape input trajectories and input torques can be obtained through a reduced set of differential equations. This approach has also yielded insight into how systems can be shown to be (partially) differentially flat.

In future work, further investigation into the structure of Eqn. (20) may provide more information on the flatness properties and feasible trajectories of subclasses of systems. We would also like to combine our formulation with current methods for non-fully actuated systems, as well as further explore the links underlying manipulation and locomotion, a potentially rich intersection as shown by the simple utility of Eqn. (26). Finally,

we hope that this work will provide motivation for further exploration of input solutions beyond periodic gaits in these systems.

REFERENCES

[1] Kelly, S. D., and Murray, R. M., 1995. "Geometric phases and robotic locomotion". *Journal of Robotic Systems,* ***12***(6), pp. 417–431.

[2] Bloch, A. M., Krishnaprasad, P., Marsden, J. E., and Murray, R. M., 1996. "Nonholonomic mechanical systems with symmetry". *Archive for Rational Mechanics and Analysis,* ***136***(1), pp. 21–99.

[3] Ostrowski, J. P., 1999. "Computing reduced equations for robotic systems with constraints and symmetries". *Robotics and Automation, IEEE Transactions on,* ***15***(1), pp. 111–123.

[4] Ostrowski, J., and Burdick, J., 1998. "The geometric mechanics of undulatory robotic locomotion". *The International Journal of Robotics Research,* ***17***(7), pp. 683–701.

[5] Ostrowski, J. P., Desai, J. P., and Kumar, V., 2000. "Optimal gait selection for nonholonomic locomotion systems". *The International journal of robotics research,* ***19***(3), pp. 225–237.

[6] Mukherjee, R., and Anderson, D. P., 1993. "Nonholonomic motion planning using Stoke's theorem". In Robotics and Automation, 1993. Proceedings., 1993 IEEE International Conference on, pp. 802–809 vol.3.

[7] Mukherjee, R., and Anderson, D. P., 1994. "A surface integral approach to the motion planning of nonholonomic systems". *Journal of dynamic systems, measurement, and control,* ***116***(3), pp. 315–325.

[8] Melli, J. B., Rowley, C. W., and Rufat, D. S., 2006. "Motion planning for an articulated body in a perfect planar fluid". *SIAM Journal on applied dynamical systems,* ***5***(4), pp. 650–669.

[9] Shammas, E. A., Choset, H., and Rizzi, A. A., 2007. "Geometric motion planning analysis for two classes of underactuated mechanical systems". *The International Journal of Robotics Research,* ***26***(10), pp. 1043–1073.

[10] Shammas, E. A., Choset, H., and Rizzi, A. A., 2007. "Towards a unified approach to motion planning for dynamic underactuated mechanical systems with non-holonomic constraints". *The International Journal of Robotics Research,* ***26***(10), pp. 1075–1124.

[11] Hatton, R. L., and Choset, H., 2011. "Geometric motion planning: The local connection, Stokes' theorem, and the importance of coordinate choice". *The International Journal of Robotics Research,* ***30***(8), pp. 988–1014.

[12] Fliess, M., Lévine, J., Martin, P., and Rouchon, P., 1995. "Flatness and defect of non-linear systems: introductory theory and examples". *International Journal of Control,* ***61***(6), pp. 1327–1361.

[13] Martin, P., Murray, R. M., and Rouchon, P., 2002. "Flat systems".

[14] Murray, R. M., Rathinam, M., and Sluis, W., 1995. "Differential flatness of mechanical control systems: A catalog of prototype systems". In ASME International Mechanical Engineering Congress and Exposition, ASME.

[15] Rouchon, P., Fliess, M., Lévine, J., and Martin, P., 1993. "Flatness, motion planning and trailer systems". In Decision and Control, 1993., Proceedings of the 32nd IEEE Conference on, IEEE, pp. 2700–2705.

[16] Murray, R. M., 1996. "Trajectory generation for a towed cable system using differential flatness". In IFAC World Congress, pp. 395–400.

[17] Murray, R. M., 1997. "Nonlinear control of mechanical systems: A lagrangian perspective". *Annual Reviews in Control,* ***21***, pp. 31–42.

[18] Bloch, A. M., 2003. *Nonholonomic mechanics and control*, Vol. 24. Springer Science & Business Media.

[19] Ramasamy, S., Wu, G., and Sreenath, K., 2014. "Dynamically feasible motion planning through partial differential flatness". In Robotics: Science and Systems.

[20] Rheinboldt, W. C., 1984. "Differential-algebraic systems as differential equations on manifolds". *Mathematics of computation,* ***43***(168), pp. 473–482.

[21] Dear, T., Hatton, R. L., Travers, M., and Choset, H., 2013. "Snakeboard motion planning with local trajectory information". In ASME 2013 Dynamic Systems and Control Conference, American Society of Mechanical Engineers, p. V002T33A002.

[22] Klein, C. A., and Huang, C.-H., 1983. "Review of pseudoinverse control for use with kinematically redundant manipulators". *Systems, Man and Cybernetics, IEEE Transactions on*(2), pp. 245–250.

[23] Yoshikawa, T., 1984. "Analysis and control of robot manipulators with redundancy". In Robotics Research: The First International Symposium, MIT press Cambridge, MA, pp. 735–747.

[24] Siciliano, B., 1990. "Kinematic control of redundant robot manipulators: A tutorial". *Journal of Intelligent and Robotic Systems,* ***3***(3), pp. 201–212.

[25] Durham, W. C., 1993. "Constrained control allocation". *Journal of Guidance, Control, and Dynamics,* ***16***(4), pp. 717–725.

[26] Bodson, M., 2002. "Evaluation of optimization methods for control allocation". *Journal of Guidance, Control, and Dynamics,* ***25***(4), pp. 703–711.

[27] Kelly, S., Fairchild, M., Hassing, P., and Tallapragada, P., 2012. "Proportional heading control for planar navigation: The Chaplygin beanie and fishlike robotic swimming". In American Control Conference (ACC), 2012, pp. 4885–4890.